



The optical and infrared study of an active star-formation region in the southern part of Mon R2

T.A. Movsessian¹, T.Yu. Magakian¹, J. Bally², A.V. Moiseev³, H.R. Andreasyan¹

¹ Byurakan Observatory of the National Academy of Sciences of Armenia, Byurakan, Aragatsotn prov., 0213, Armenia
e-mail: tigmov@bao.sci.am

² Department of Astrophysical and Planetary Sciences, University of Colorado, Boulder, CO, USA

³ Special Astrophysical Observatory, Nizhny Arkhiz, Karachaevo-Cherkesia, 369167 Russia
e-mail: moi.sav@sao.ru

Received 28 November 2022

ABSTRACT

This is a shortened version of the presentation at the conference “Non-Stationary Processes in the Protoplanetary Disks and Their Observational Manifestations” held at the Crimean Astrophysical Observatory.

We present narrow-band images of the southern part of the Mon R2 association obtained in the course of the BNBIS survey with the 1-m Schmidt telescope of the Byurakan Observatory. The main task of this survey is search and study of new Herbig-Haro (HH) objects and collimated outflows using the narrow-band H_α and [S II] images of certain fields in dark clouds of the Galaxy since the presence of HH objects is one of the main indicators of active star-formation processes.

Several new HH objects and outflow systems were discovered, including the helical chain of HH objects near IRAS 06068-0643 (V963 Mon) and the curved outflow system associated with the 2MASS 06084223-0657385 source, which probably represents the irradiated giant outflow. Also, two molecular hydrogen outflows associated with deeply embedded IR sources near the 2MASS 06084223-0657385 region were revealed.

Key words: YSO's, Herbig-Haro objects, outflows

1 Introduction

The Mon R2 association is one of the well-known star-forming regions, which was identified as a large cluster of nine reflection nebulae by [Van den Bergh \(1966\)](#). Besides of illuminating stars of spectral types B1–B9, it contains a number of pre-main-sequence (PMS) objects ([Herbst, Racine, 1976](#); [Herbig, Bell, 1988](#); [Porrás et al., 2003](#)) and several HH objects ([Carballo, Eiroa, 1992](#); [Wang et al., 2005](#)).

This association is located in the large molecular cloud L1646 at a distance of 830 pc ([Herbst, Racine, 1976](#)), which extends over $3^\circ \times 6^\circ$ and has a total mass of $9 \times 10^4 M_\odot$ ([Maddalena et al., 1986](#)).

Our attention was focused on a region of about $30'$ south from the center of Mon R2, which is less studied but contains several nebulous objects including the V899 Mon eruptive star with spectral features of both FUors and EXors ([Ninan et al., 2015](#); [Park et al., 2021](#)). Besides, not far from V899 Mon, there are some nebulous infrared sources associated with characteristic cone-shaped reflection nebulae.

This work was performed in the frame of the Byurakan Narrow Band Imaging Survey (BNBIS) started with the 1-m Schmidt telescope of the Byurakan Observatory in order to find new HH objects and collimated outflow systems ([Movsessian et al., 2020](#)).

Additionally, we present the narrow-band H_α as well as near-IR observations carried out with the 3.5-m telescope of the Apache Point Observatory (APO).

2 Observations

2.1 Optical range

Images were obtained on the nights of 21–27 January 2020 with the 1-m Schmidt telescope of the Byurakan Observatory equipped with the re-worked $4K \times 4K$ Apogee liquid-cooled CCD camera providing a 1-deg field of view with a resolution of $0.868''$ per pixel ([Dodonov et al., 2017](#)).

The narrow-band filters centered on 6560 \AA and 6760 \AA , both with a FWHM of 100 \AA , were used to obtain the H_α and [S II] images, respectively. A mid-band filter centered on 7500 \AA with a FWHM of 250 \AA was used for continuum imaging.

The dithered sets of 5-min exposures were obtained in each filter. The effective exposure in H_α was 8300; in [S II] and continuum, 5400 and 2400 seconds, respectively. Images were reduced in the standard manner using the IDL package, which includes bias subtraction, cosmic ray removal, and flat-fielding using a “super flat”.

2.2 Infrared range

Observations were carried out with the APO ARC 3.5-m telescope equipped with the NIC-FPS instrument. The Rockwell Hawaii 1-RG 1024×1024 HgCdTe device with a $0.273''/\text{pixel}$ scale and $4.58'$ square, unvignetted field, and sensitivity from 0.85 to $2.4 \mu\text{m}$ was used as a detector. The actual exposure time in the H_2 $2.12 \mu\text{m}$ filter was 180 seconds.

2.3 Long-slit spectroscopy

Spectral observations were performed with the 6-m telescope of the Special Astrophysical Observatory using the SCORPIO-2 (Afanasiev et al., 2017) multi-mode focal reducer mounted in the primary focus of the telescope. The CCD261-84 of 2048×4104 pixels and the $15 \times 15 \mu\text{m}$ pixel size was used as a detector. To increase the S/N ratio, a data binning of 1×2 in the long-slit mode was applied, providing the $0.2 \times 0.4''$ image scale. The field of view was $6.1'$ with a scale of $0.2''$ per pixel. During the observation, the VPHG1200@540 grism in a wavelength range of $3650\text{--}7300 \text{ \AA}$ was used. The spectral resolution was about 5.2 \AA across the full range of wavelengths (the mean reciprocal dispersion was $0.89 \text{ \AA}/\text{px}$) and a spatial scale of $0.4''$ per pixel along the slit.

3 Results

3.1 Optical and near-IR images

Figure 1 shows an $\text{H}\alpha + [\text{S II}]$ image of the studied field in the Mon R2 region obtained with the 1-m Schmidt telescope. The regions with newly discovered HH objects and HH outflows are marked by two rectangles. The first region is located near V899 Mon and the second one, near the 2MASS 06084223-0657385 source associated with a bipolar reflection nebula. Besides, we obtain NIR images in the molecular hydrogen (H_2) line for the 2MASS 06084223-0657385 region using the ARC 3.5-m telescope.

The descriptions of separate objects and groups are given below.

3.1.1 V899 Mon region

Figure 2 presents images of the region near V899 Mon that show its appearance in the continuum and emission lines. Their comparison shows that in the vicinity of V899 Mon itself no emission knots in $\text{H}\alpha$ images can be seen, but in the $[\text{S II}]$ lines a narrow and very faint jet-like structure oriented along the axis of the associated reflection nebula is barely visible (compare the upper right and lower right panels in Fig. 2). This structure starts at a distance of about $42''$ NE from V899 Mon and has a length of about $11''$. Of course, the reality of this jet should be confirmed by images with higher limit and spatial resolution.

Besides, new HH objects were discovered at a distance of about $2.5'$ SW from V899 Mon, near the IRAS 06068-0643 source, which is also known as V963 Mon. This star is associated with a compact reflection nebula and shows spectral features and photometric variability typical of EXors

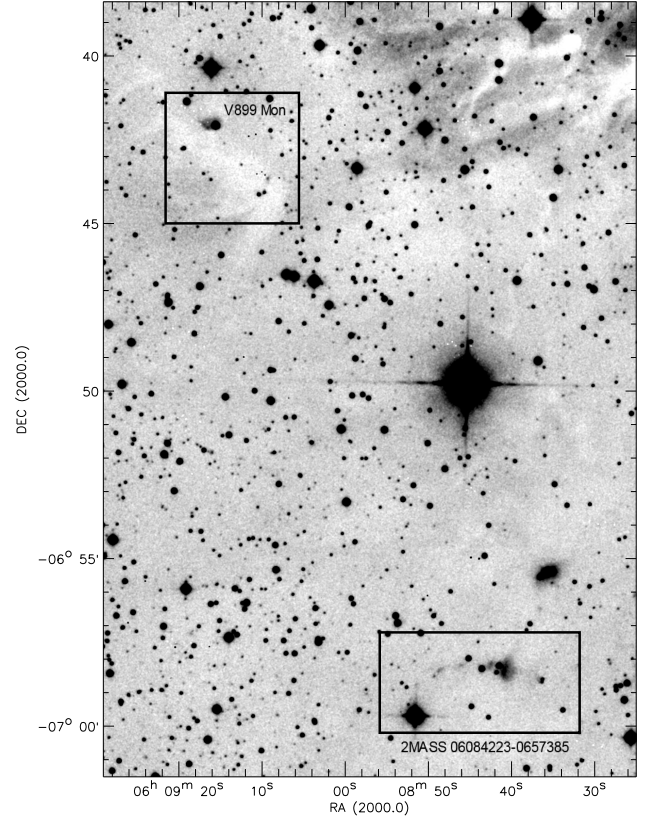


Fig. 1. Part of the 1-deg field of the Byurakan Schmidt telescope with newly discovered HH objects and outflows shown by rectangles ($\text{H}\alpha + [\text{S II}]$ emission).

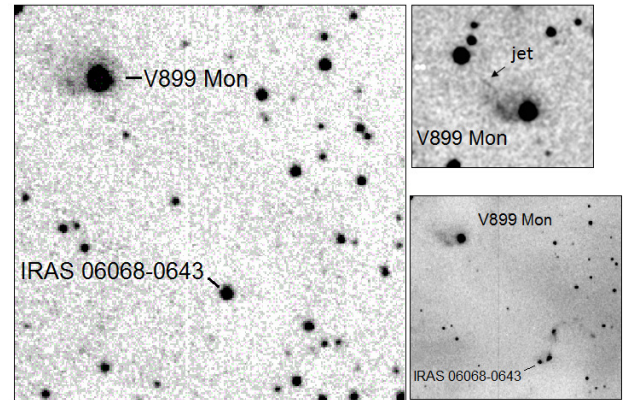


Fig. 2. The V899 Mon field in the continuum (left panel), in $[\text{S II}]$ (upper right) and $\text{H}\alpha$ (lower right). The helical chain of HH objects near IRAS 06068-0643 is clearly seen.

(Wils et al., 2009). In the $\text{H}\alpha$ image, the chain of HH knots near this source can be seen. The higher resolution image of the same region obtained with the APO ARC telescope in the $\text{H}\alpha$ line reveals the faint emission filament with a helical structure, which starts from the V963 Mon star and connects all HH knots (see Fig. 2, lower right panel).

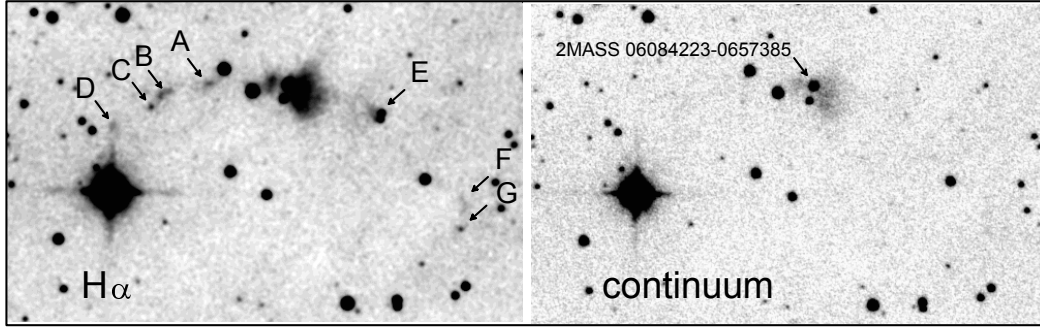


Fig. 3. The $H\alpha$ (left panel) and continuum images (right panel) of the curved jet associated with the 2MASS 06084223-0657385 source.

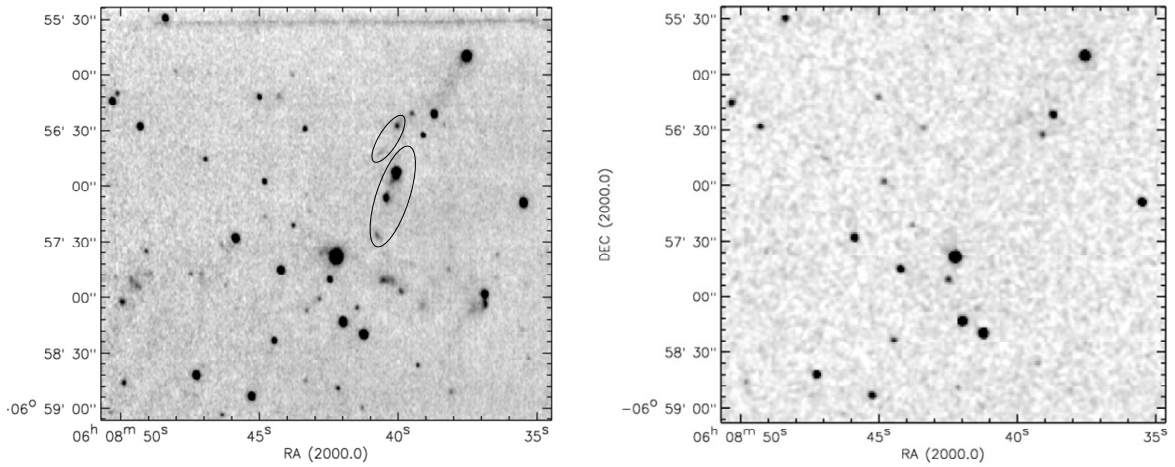


Fig. 4. Near-IR images of the 2MASS 06084223-0657385 region in $2.12 \mu\text{m}$ (H_2 emission) (left panel) and in the 2MASS K-band (right panel). New MHOs are marked by ellipses.

3.1.2 2MASS 06084223-0657385 region

In about $20'$ south-west direction from V899 Mon, we revealed several HH knots near the 2MASS 06084223-0657385 IR source associated with a biconic reflection nebula. These newly discovered HH objects trace a parabolic curve at the apex of which the IR source is located (see Fig. 3, left panel). Thus, it is obvious that here we can observe a bipolar outflow with an unusual arc-shaped structure. Such a morphology is typical of the so-called irradiated jets (Bally, Reipurth, 2001). In this particular case, the outflow can be irradiated by the Lyman continuum and/or softer far-ultraviolet radiation of high-mass stars located in the center of the Mon R2 association.

For the distance of 900 pc, the estimated total length of this bipolar outflow will be about 1.5 pc, which means that this outflow system belongs to the so-called giant or parsec-scale HH outflows.

In this field, new molecular hydrogen flows were also discovered. In fact, all HH knots in the parabolic chain described above are also visible in the H_2 $2.12 \mu\text{m}$ line. Besides, at a distance of $1'$ north from it, we found two previously unknown molecular hydrogen flows that have no optical counterparts. Their probable sources are the 2MASS 06083754-0655496 object, which is associated with a faint cone-shaped reflec-

tion nebula visible even in the optical range, and the deeply embedded source WISE J060839.50-065620.7. These two flows consist of elongated linear chains of knots, whose axes pass through these sources. They are marked by ellipses in Fig. 4 (left panel). Their emission nature is confirmed by their invisibility in the 2MASS K-band image (see Fig. 4, right panel).

3.2 Long-slit spectroscopy

We also obtained a long-slit spectrum of the 2MASS 06084223-0657385 flow, orienting the slit in the EW direction through the source and the cone-shaped bipolar reflection nebula. Figure 5 (left panel) shows a two-dimensional spectrum. The pure emission nature of knots in this system is obvious. Moreover, at a distance of $7''$ west from the source, a new HH knot was found, which is not visible in direct images due to the bright background of the reflection nebula. The right panel of Fig. 5 presents the position-velocity diagram (PV) in the [SII] lines. As can be seen from the PV diagram, the radial velocities in the eastern and western directions from the source have the opposite sign, which confirms the bipolar nature of this outflow system. The western wing has positive velocity (about $+40 \text{ km s}^{-1}$) and the eastern one, negative (about -40 km s^{-1}).

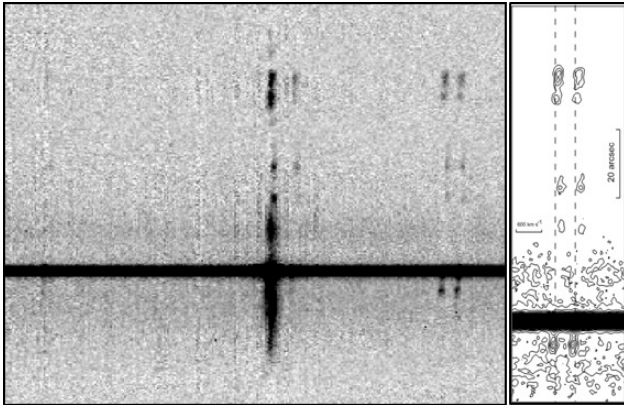


Fig. 5. Part of the long-slit spectrum near the $H\alpha$ and $[SII]$ lines (left panel) and the PV diagram of $[SII]$ emissions (right panel).

4 Conclusions

This work is part of the Byurakan Narrow Band Imaging Survey (BNBIS). Taking into account all results obtained during this survey, we can emphasize the high efficiency of the 1-m Schmidt telescope of the Byurakan Observatory equipped with a CCD detector and high-quality narrow-band filters. Below we summarize our findings.

- We discovered a curved HH outflow associated with the 2MASS 06084223-0657385 source; its curvature can result from radiation pressure of luminous stars located near the center of the Mon R2 association.
- Long-slit spectroscopy confirmed the bipolar nature of this outflow and allowed us to reveal another HH knot near the central source, against the background of the bright reflection nebula.
- The narrow jet on the axis of the reflection nebula associated with V899 Mon was discovered.
- The unique helical chain of HH objects near the IRAS 06068-0643 star was found.

- In the NIR images of the H_2 line, several new molecular knots were found, including the HH knots in the parabolic chain and two flows associated with 2MASS 06083754-0655496 and the deeply embedded source WISE J060839.50-065620.7.

This work was partly supported by the RA State Committee of Science in the frame of the research project No. 21T-1C031.

References

- Afanasiev V.L., Amirkhanyan V.R., Moiseev A.V., et al., 2017. *Astrophys. Bull.*, vol. 72, p. 458.
- Bally J., Reipurth B., 2001. *Astrophys. J.*, vol. 546, p. 299.
- Carballo R., Eiroa C., 1992. *Astron. Astrophys.*, vol. 262, p. 295.
- Dodonov S.N., Kotov S.S., Movsesyan T.A., Gevorkyan M., 2017. *Astrophys. Bull.*, vol. 72, p. 473.
- Herbig G.H., Bell K.R., 1988. Third catalog of emission-line stars of the Orion population, *Lick Obs. Bull.*, no. 1111, Santa Cruz: Lick Observatory.
- Herbst W., Racine R., 1976. *Astron. J.*, vol. 81, p. 840.
- Maddalena R.J., Morris M., Moscowitz J., Thaddeus P., 1986. *Astrophys. J.*, vol. 303, p. 375.
- Movsessian T.A., Magakian T.Y., Dodonov S.N., et al., 2020. *Commun. Byurakan Astrophys. Observatory*, vol. 67, p. 257.
- Ninan J.P., Ojha D.K., Baug T., et al., 2015. *Astrophys. J.*, vol. 815, p. 4.
- Park S., Kóspál Á., Cruz-Sáenz de Miera F., et al., 2021. *Astrophys. J.*, vol. 923, p. 171.
- Porras A., Christopher M., Allen L., et al., 2003. *Astron. J.*, vol. 126, p. 1916.
- Racine R., 1968. *Astron. J.*, vol. 73, p. 233.
- Van den Bergh S., 1966. *Astron. J.*, vol. 71, p. 990.
- Wils P., Greaves J., Drake A.J., et al., 2009. *Central Bureau Electronic Telegrams*, No. 2033.
- Wang H., Stecklum B., Henning T., 2005. *Astron. Astrophys.*, vol. 437, p. 169.